Experimental Study of Sliding Isolated Structures with Uplift Restraint

By Satish Nagarajaiah,[1] Associate Member, ASCE, Andrei M. Reinhorn,[2] Member, ASCE, and Michalakis C. Constantinou,[3] Associate Member, ASCE

Abstract: An experimental study, performed to evaluate the feasibility of using a sliding isolation system with uplift restraint devices for medium-rise buildings subject to column uplift, is presented. A Teflon-disc sliding bearing with built-in uplift restraint devices is described. A quarter-scale, 52-kip (231-kN) model of a six-story structure was isolated using the sliding isolation system with uplift restraint devices. The model had a slender configuration with ratio of height to width of 4.5. The slender configuration was chosen to ensure column uplift. Shake-table tests, involving strong motions with different frequency contents and peak table accelerations as high as 0.6 g, were performed. The shake-table test results show that the sliding isolation system is effective in reducing the structural response and uplift forces, by reducing the lateral floor accelerations and overturning moments, and that the uplift restraint system is effective in resisting uplift forces. An analytical model for predicting the response is developed. Comparisons between the predicted and observed responses are presented.

Introduction

A slender, nonisolated medium-rise building, with a large aspect ratio of height to width, can generate overturning moments large enough to cause partial uplift in portions of the building. Partial uplift is not necessarily harmful and may lead to better performance of tall structures during earthquakes (Housner 1963). Tall bridge piers have been designed to rock about their bases to take advantage of the beneficial effects of base uplift (Beck and Skinner 1974). Experimental study of uplift in model steel frames, representing medium-rise buildings, revealed that partial uplift may result in reduced strength and ductility requirements on the frame (Huckelbridge and Clough 1978). Analytical studies on the response of uplifting flexible systems have been performed by many researchers (Chopra and Yim 1985; Psycharis 1990; Wolf 1976; Meek 1975; Priestly et al. 1978). These analytical studies found that partial uplift of the base leads to reduction of the structural deformations and forces, compared with the fixed-base response, for a wide range of structural periods. From the aforementioned studies, it is evident that partial uplift may be allowed to occur, provided that the magnitude of the uplift displacement is kept within limits, barring which impact on contact may severely damage the elements involved. In all these studies, nonisolated structures were considered, and no sliding occurred at the structure-foundation interface.

The use of base isolation systems (Kelly 1988; Buckle and Mayes 1990), such as elastomeric or sliding systems, to isolate the structure can reduce

[1]Res. Asst. Prof., Dept. of Civ. Engrg., State Univ. of New York, Buffalo, NY 14260.

[2]Prof., Dept. of Civ. Engrg., State Univ. of New York, Buffalo, NY.

[3]Assoc. Prof., Dept. of Civ. Engrg., State Univ. of New York, Buffalo, NY.

Note. Discussion open until November 1, 1992. To extend the closing date one month, a written request must be filed with the ASCE Manager of Journals. The manuscript for this paper was submitted for review and possible publication on June 10, 1991. This paper is part of the ***Journal of Structural Engineering***, Vol. 118, No. 6, June, 1992. ©ASCE, ISSN 0733-9445/92/0006-1666/$1.00 + $.15 per page. Paper No. 2093.

the overturning moments and uplift forces by providing flexibility and energy dissipation capacity at the structure-foundation interface. The reduction in uplift forces, due to the reduction of the lateral floor accelerations, is substantial, yet the uplift forces can be large enough to be of concern. In such cases, uplift restraint devices are employed to resist the uplift forces and prevent large uplift displacements. The isolation bearings, either elastomeric or sliding bearings, cannot resist uplift forces. Furthermore, if large uplift displacements are not prevented, loss of contact and eventual impact on contact leads to higher-mode response and large axial forces in columns. Also, the sudden increase in the axial force in the bearings may lead to local instability of the bearings.

The effectiveness of uplift restraint devices in alleviating the problem of uplift in base-isolated structures with elastomeric isolation systems has been demonstrated by means of shake-table tests (Griffith et al. 1990). The tested system was a nine-story model, with an aspect ratio of height to width of 1.6, on elastomeric bearings with uplift restraint devices. Base-isolated structures, with aspect ratios ~ 3, on elastomeric isolation systems with uplift restrainers have been built in Japan (Kelly 1988; Buckle and Mayes 1990).

Uplift restraint devices have also been used in base-isolated structures with sliding isolation systems. The friction pendulum system with uplift restraint devices (Zayas et al. 1989) was used for isolating a slender, 50,000-gal. water tank in California. The Olympic Saddle Dome Stadium in Calgary, Alberta, Canada, rests on multidirectional sliding bearings with built-in uplift restrainers (*Wabo-Fyfe* 1990).

In this paper, an experimental study of a slender model structure on a sliding isolation system with uplift restraint devices is reported. Shake-table tests were performed on a quarter-scale model of a six-story steel-braced frame, in which the aspect ratio of height to width was 4.5. The sliding isolation system consisted of sliding bearings augmented with uplift restraint devices to resist uplift forces.

The purpose of the experimental study was to evaluate the feasibility of using a sliding isolation system with uplift restraint devices for medium-rise buildings subject to column uplift. Furthermore, an extreme aspect ratio of 4.5 was chosen to ensure column uplift, since the effect of column uplift on the response of sliding isolated structures was of interest. The shake-table tests involved several simulated earthquake motions, with significantly different frequency content and peak accelerations as high as 0.6 g. The test results demonstrated the effectiveness of the sliding isolation system with uplift restrain devices in reducing the overturning moments and resisting the uplift forces.

This paper also presents the analytical prediction of the observed response. The analytical model presented includes rocking and variation of coefficient of fricition with velocity and bearing pressure. The analytical predictions match the observed response closely.

Test Structure

The tested model was a steel frame six stories tall, one bay wide and braced in the weak direction (the direction of testing), as shown in Fig. 1. The model had three bays of moment-resisting frame in the strong direction, as shown in Fig. 1. Concrete blocks were added to satisfy mass similitude requirements, and the resulting model weight was 51.4 kips (229.2 kN). The distribution of weight with height was 7.65 kips (34.1 kN) at the sixth floor,

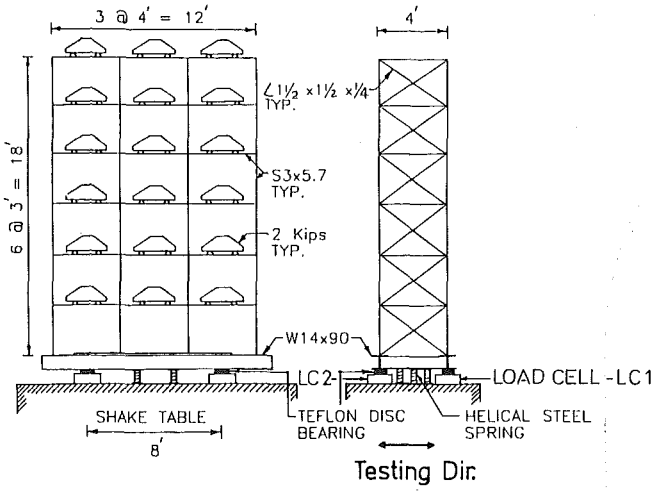

FIG. 1. Test Structure Elevation in Testing Direction and Direction Perpendicular to Testing Direction (1 ft = 304.8 mm; 1 kip = 4.45 kN)

7.84 kips (34.9 kN) at the fifth to first floors, and 4.56 kips (20.3) at the base. The model was fixed to a base of two W14 X 90 sections. The isolation system was placed between the base and the shake table.

The test structure was instrumented with a combination of accelerometers, linear potentiometers, sonic displacement transducers, and load cells to record the response of the structure for all input excitations. The axial force, shear force, and moment at the bearing level were measured using load cells placed below the sliding bearings. The shake-table rocking input due to shake-table–structure interacton was measured by means of two vertical accelerometers placed at the ends of the shake table in the testing direction. The vertical or uplift displacements at the sliding bearings were measured by potentiometers connecting the top and bottom plate of the sliding bearings. The vertical displacement measurements were made at two bearing-load cell locations (load cell LC1 and LC2, see Fig. 1 for details) in the test direction, so that the vertical displacement in both cycles of the structural response could be measured.

Sliding Isolation System and Uplift Restraint Devices

The isolation system considered (Constantinou et al. 1991) consisted of four sliding Teflon-disc bearings, which were placed between the base and the heavy-duty load cells resting on the shake table, and helical spring units, which were placed between the base and the shake table, as shown in Fig. 1. The Teflon-disc bearing with uplift restraint devices and the helical spring unit are shown in Fig. 2. The upper steel plate of the bearing is faced with a polished stainless-steel plate underneath. The lower steel plate of the bearing has an unfilled Teflon disc, 2.8 in. (71.1 mm) in diameter, recessed on its top. The lower steel plate is supported by a high-hardness Adiprene (urethane rubber) disc. The lower plate is held by a shear-uplift restriction mechanism. The Adiprene disc allows some limited rotation and vertical displacement of the lower steel plate, so that full contact is maintained

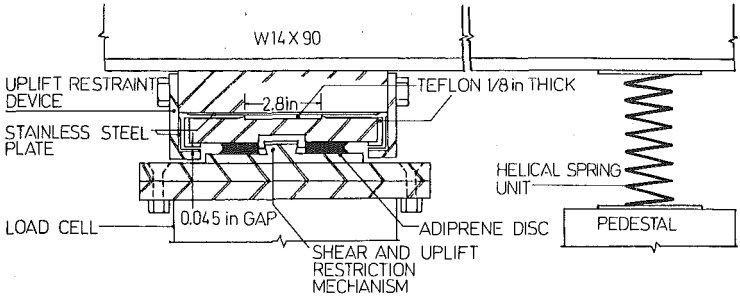

FIG. 2. Section of Teflon Disc Bearing with Uplift Restraint Devices, Perpendicular to Testing Direction, and Helical Spring Unit (1 in. = 25.4 mm)

between the polished stainless-steel plate and the Teflon disc. The bearing allows 2.8 in (71.12 mm) of movement from the center of the bearing (i.e., a total movement of 5.6 in., or 142.24 mm) in the testing direction. The inside part of the uplift restraint device is faced with polished stainless-steel plate. The lower steel plate has Teflon sheet facing on the sides as well as the bottom, so that when the uplift restraint devices engage the horizontal movement in the testing direction occurs smoothly (see Fig. 2 for details). Fig. 2 shows the gaps between the lower steel plate and the uplift restraint device—a horizontal gap of 0.25 in. (6.35 mm) that allows limited movement in the direction perpendicular to the testing direction and a vertical gap of 0.045 in. (1.14 mm) that allows limited vertical movement before the uplift restraint devices engage with the lower steel plate.

The load cells supporting the bearings had 50 kips (222.4 kN) of axial load capacity per load cell. The load cells were placed on top of the leveling plates resting on top of the shake table. The leveling plates were leveled with a system of bolts, and the load cells were bolted down to the shake table and grouted in this position. The upper plate of each bearing was leveled by the following procedure. A washer was placed between the plate and the W14 X 90 section above, and the four connecting bolts were used to level the plate. In this position, the plate was grouted. Measurements of the inclination of the plates revealed that, on an average, the four sliding plates were inclined by 0.5° in the testing direction.

The helical steel-spring units (see Figs. 1 and 2) provided the restoring force or recentering capability. The spring units, attached to the base and pedestals on the shake table, carried a total compressive load of 1.4 kips (6.23 kN), with the remaining weight of the model carried by the four sliding bearings. Each spring unit consisted of three helical springs with a length of 7.5 in. (190.5 mm), external diameter of 3.1 in. (78.7 mm), and wire diameter of 0.512 in. (13 mm). The spring units provided restoring force or recentering capability by deforming in shear. The measured stiffness characteristics of the system with four spring units were nonlinear elastic with: (1) A stiffness of 1.54 kips/in. (0.27 kN/mm) to 0.5 in. (12.7 mm); and (2) a stiffness of 2.68 kips/in. (0.47 kN/mm) beyond 0.5 in.(12.7 mm) displacement.

The rigid body mode period T_b of the sliding base-isolated structure, considering only the stiffness of the springs and disregarding the frictional force, is defined as follows:

$$T_b = 2\pi \left(\frac{W}{gK_2}\right)^{1/2} \quad \ldots\ldots (1)$$

where W = weight of the structure and K_2 = stiffness of the spring units beyond 0.5 in. (12.7 mm) of displacement. T_b in the tested system was 1.4 sec when four spring units (with three springs per unit) were used; 1.98 sec with two spring units (with three springs per unit); and infinite when no spring units were used.

The coefficient of friction at a Teflon-steel interface depends on the velocity and the bearing pressure. The coefficient of friction can be modeled by the following equation (Constantinou et al. 1990):

$$\mu = f_{\max} - \Delta f \times \exp(-a|\dot{U}_b|) \quad \ldots\ldots (2)$$

where $\dot{U}_b$ = the velocity at the sliding interface; $f_{\max}$ = maximum coefficient of friction; Δf = the difference between maximum and minimum coefficients of friction; and a = constant governing the variation betwen maximum and minimum coefficients of friction. During the tests under various earthquakes, the values of $f_{\max}$ varied between 0.1 and 0.14, and the values of Δf varied between 0.03 and 0.06, with a = 0.55 sec/in. (21.6 sec/m). For these values of coefficients of friction, the mobilized peak frictional force = 7 kips (31.1 kN). The peak restoring force due to the four helical spring units = 4.8 kips (21.3 kN) for a peak displacement of 2 in. (50.8 mm). Hence, the ratio of peak frictional force to peak restoring force indicates a sliding system with weak restoring force.

Test Program

The test program consisted of free-vibration tests, white-noise input tests, and earthquake input tests. The first two types of tests were performed to determine the dynamic characteristics of the fixed-base model. Only lateral earthquake excitation was applied, and no vertical excitation was applied. The shake-table–structure interaction resulted in rocking accelerations at the shake-table level. These rocking accelerations were monitored carefully, with appropriate instrumentation described earlier.

Several earthquakes were used to excite the structure on the shake table. The earthquake characteristics ranged from predominantly low-frequency ground motion (Mexico city, Hachinohe) to moderately high-frequency ground motion (El Centro, Miyagiken-Oki). The records were time scaled by a factor of two to satisfy similitude requirements. Each earthquake was applied with increasing levels of peak table acceleration until the model lifted off the two bearings on one side and the uplift restraint devices were clearly engaged during the test runs. The earthquake signals used were as follows:

1. Imperial Valley earthquake (El Centro S00E), May 18, 1940; component S00E; peak ground acceleration (PGA) = 0.34 g; predominant frequency range (PFR) = 1–4 Hz.
2. San Fernando earthquake (Pacoima S74W), February 9, 1971; component S74W; PGA = 1.08 g; PFR = 0.25–2 Hz.
3. San Fernando earthquake (Pacoima S16E), February 9, 1971; component S16E; PGA = 1.17 g; PFR = 0.25–6 Hz.
4. Kern County earthquake (Taft N21E), July 21, 1952; component N21E; PGA = 0.16 g; PFR = 0.5–5 Hz.

5. Miyagiken-Oki earthquake (Miyagiken-Oki: Tohoku University, Sendai, Japan), June 12, 1978; component EW; PGA = 0.16 g; PFR = 0.5–5 Hz.
6. Tokachi-Oki earthquake (Hachinohe: Japan), May 16, 1968; component NS; PGA = 0.23 g; PFR = 0.25–1.5 Hz.
7. Mexico City earthquake (Mexico City N90W: SCT building station), September 19, 1985; component N90W; PGA = 0.17 g; PFR = 0.35–0.55 Hz.

Dynamic Characteristics of Test Structure

The natural frequencies, damping ratios, and mode shapes of the model structure in the braced direction under fixed-base conditions, listed in Table 1, were determined experimentally. Compensated white noise (0–50 Hz) of 0.04 g peak table acceleration was used for system identification. The absolute acceleration transfer functions of the six floors of the fixed-base model were used for determining the structural parameters by modal identification techniques (Nagarajaiah et al. 1992). The results of the first-mode frequency and damping were confirmed further by pull-back tests resulting in free vibration. The measured rocking frequency was 3.4 Hz in the isolated condition.

Test Results

A summary of the experimental results is shown in Tables 2 and 3. The model remained elastic in all tests. No torsional motions were observed in the tests. Tables 2 and 3 show the excitation used in the test program, the isolation system condition, the peak table acceleration, and the maximum response of the model in terms of the peak bearing displacement, ratio of the base shear over total weight of 51.4 kips (229.2 kN), peak base acceleration, peak model acceleration, the ratio of peak interstory drift over story height, peak bearing uplift displacement, and permanent bearing displacement at the end of free-vibration response. Four isolation conditions are identified in Table 2. Fixed for fixed-base condition and SB4HS, SB2HS, and SB0HS for the sliding system with four, two, and no helical spring units, respectively (note: SB stands for sliding bearing, HS stands for helical spring units, and the number specifies the number of helical spring units). The earthquake excitation in Tables 2 and 3 is presented with a percentage figure that applies to the PGA of the actual record. For example, in the case of Miyagiken-Oki, 300% corresponds to the actual Miyagiken-Oki record with peak acceleration increased approximately by a factor of three. The input

TABLE 1. Dynamic Characteristics of Structure Under Fixed-Base Conditions

Mode (1)	Frequency (Hz) (2)	Damping ratio (3)	Mode Shape: Floor six (top) (4)	Floor five (5)	Floor four (6)	Floor three (7)	Floor two (8)	Floor one (9)
1	3.63	0.0178	1	0.881	0.709	0.560	0.401	0.217
2	15.25	0.0104	−0.944	−0.249	0.501	0.822	1	0.583
3	21.87	0.0069	0.825	−0.412	1	−0.268	0.771	0.825
4	27.74	0.0183	0.172	−0.1	−0.328	0.245	0.450	−1
5	35.5	0.0058	0.503	−0.899	0.099	0.901	−1	0.102
6	47.2	0.0034	−0.202	0.499	−0.601	0.503	−1	0.404

TABLE 2. Summary of Experimental Results

Excitation (1)	Isolation conditions (2)	Peak Model Response Value: Table acceleration (g) (3)	Bearing displacement (in) (4)	Base shear[a]/ weight (5)	Base acceleration (g) (6)	Floor[b] acceleration (g) (7)	Interstory drift[b]/ story height (8)	Bearing uplift displacement[c] (in.) (9)	Permanent displacement (in.) (10)
El Centro S00E 30%	Fixed	0.13	—	0.200	—	0.52 (6)	0.0022 (6)	—	—
El Centro S00E 65%	SB0HS	0.22	0.586	0.133	0.28	0.33 (6)	0.0013 (6)	0.023	0.586
El Centro S00E 65%	SB2HS	0.22	0.334	0.132	0.27	0.32 (6)	0.0013 (6)	0.024	0.068
El Centro S00E 65%	SB4HS	0.22	0.346	0.132	0.26	0.32 (6)	0.0011 (6)	0.024	0.035
El Centro S00E 100%	SB4HS	0.33	0.544	0.137	0.32	0.37 (6)	0.0013 (6)	0.067	0.031
El Centro S00E 125%	SB4HS	0.41	0.890	0.154	0.38	0.42 (6)	0.0017 (6)	0.076	0.06
Mexico N90W 80%	SB4HS	0.14	0.908	0.122	0.20	0.25 (6)	0.0014 (6)	0.014	0.01
Mexico N90W 100%	SB4HS	0.16	1.654	0.146	0.23	0.27 (6)	0.0013 (6)	0.028	0.02
Pacoima S74W 15%	Fixed	0.15	—	0.210	—	0.55 (6)	0.0023 (6)	—	—
Pacoima S74W 50%	SB4HS	0.39	0.297	0.125	0.33	0.39 (6)	0.0014 (6)	0.043	0.02
Pacoima S74W 70%	SB4HS	0.55	0.766	0.135	0.47	0.50 (6)	0.0016 (6)	0.105	0.03
Pacoima S74W 75%	SB4HS	0.58	0.913	0.159	0.58	0.54 (6)	0.0027 (6)	0.124	0.07

[a]Shear at bearing level.

[b]Value in parentheses is the floor at which the maximum was recorded.

[c]Peak uplift displacement among bearings located on top of load cells LC1 and LC2.

TABLE 3. Summary of Experimental Results

Excitation (1)	Isolation conditions (2)	Peak Model Response Value: Table acceleration (g) (3)	Bearing displacement (in.) (4)	Base shear[a]/ weight (5)	Base acceleration (g) (6)	Floor[b] acceleration (g) (7)	Interstory drift[b]/ height (8)	Bearing uplift displacement[c] (in.) (9)	Permanent displacement (in.) (10)
Pacoima S16E 35%	SB4HS	0.33	0.658	0.131	0.29	0.33 (6)	0.0017 (6)	0.025	0.143
Pacoima S16E 50%	SB4HS	0.46	1.126	0.144	0.41	0.40 (6)	0.0018 (6)	0.036	0.049
Hachinohe NS 100%	SB4HS	0.22	0.520	0.135	0.32	0.29 (6)	0.0010 (6)	0.025	0.107
Hachinohe NS 150%	SB4HS	0.31	1.43	0.150	0.39	0.33 (6)	0.0019 (6)	0.037	0.130
Miyagiken-Oki EW 100%	SB4HS	0.16	0.061	0.097	0.17	0.26 (6)	0.0009 (6)	0.010	0.060
Miyagiken-Oki EW 200%	SB4HS	0.33	0.247	0.125	0.27	0.30 (6)	0.0011 (6)	0.014	0.067
Miyagiken-Oki EW 300%	SB4HS	0.46	0.365	0.133	0.39	0.41 (6)	0.0015 (6)	0.032	0.005
Taft N21E 150%	SB4HS	0.28	0.266	0.126	0.25	0.30 (6)	0.0011 (6)	0.020	0.143
Taft N21E 300%	SB4HS	0.46	1.089	0.144	0.42	0.39 (6)	0.0015 (6)	0.043	0.012

[a]Shear at bearing level.

[b]Value in parentheses is the floor at which the maxium was recorded.

[c]Peak uplift displacement among bearings located on top of load cells LC1 and LC2.

signals were not compensated (except for the 0–50 Hz white noise used for identification of the system properties).

Effectiveness of System

The effectiveness of the isolation system in reducing the structural response is evident when the responses in the following cases are considered:

1. Fixed base with El Centro S00E 30% excitation, and isolated case SB4HS with El Centro S00E 125% excitation.
2. Fixed base with Pacoima S74W 15% excitation, and isolated case SB4HS with Pacoima S74W 75% excitation.

Motions with lower peak table accelerations were chosen for the fixed-base case to ensure that the model remained elastic without damage. Motions with larger peak table accelerations would have yielded the fixed-base model. In case 1, the peak interstory drift, normalized with respect to the story height, was 0.0022 in the fixed-base case and 0.0017 in the isolated case (see Table 2). In case 2, the normalized peak interstory drift was 0.0023 in the fixed-base case and 0.0027 in the isolated case (see Table 2). Hence, the capacity of the frame, with sliding isolation sytem, to withstand the El Centro and Pacoima ground motions without damage has been increased by at least a factor of three, compared with the fixed-base case. The normalized peak interstory drift is a better measure of the effectiveness of the sliding systems (Constantinou et al. 1991).

Effect of Restoring Force

Shake-table test results of a sliding isolated structure, with weak restoring force and without uplift restraint system (Constantinou et al. 1991), have revealed that the purpose of the helical spring units is to control the bearing and permanent displacements within acceptable limits and not to shift the frequencies of the structure. In essence, the presence of a different number of spring units does not change the frequency characteristics of the system. The test results of El Centro 65% with four, two, and no spring units (SB4HS, SB2HS, and SB0HS) indicate that the response (see Table 2) was almost identical in all three cases, except for the bearing and permanent displacements. The frequency content of the response was almost identical in all of the preceding cases. Loss of contact at sliding bearings occurred in all three cases, with almost identical uplift displacement.

Results of Uplift Tests

The vertical elastic deformation of the Adiprene disc in each of the sliding bearings under the weight of 12.5 kips (55.6 kN) was 0.02 in. (0.508 mm). An axial or normal force per bearing of 12.5 kips (55.6 kN) was measured by the load cells. This axial force per bearing can be determined by subtracting 1.4 kips (6.23 kN) compressive force carried by the spring units from the total weight of 51.4 kips (228.6 kN) and distributing the remaining 50 kips (222.4 kN) force to the four bearings. The model uplifted from the bearings, or lost contact, when the vertical uplift displacement exceeded 0.02 in. (0.508 mm). The engagement of the uplift restraint devices occurred when the vertical uplift displacement exceeded 0.065 in. (i.e., 0.045 in. + 0.02 in. = 0.065 in. or 1.65 mm).

Figs. 3 and 4 show: (1) The recorded base (bearing) displacement time history; (2) the base shear-displacement loops (base shear corresponds to the force at the bearing level); (3) the structure shear (in the first story

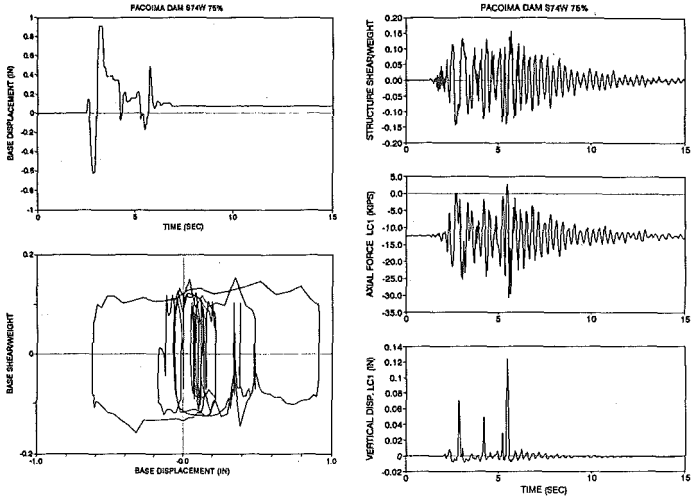

FIG. 3. Measured Response of System with Four Spring Units for Pacoima Dam Input with Peak Table Acceleration of 0.58 g; The Time Histories Shown are for Base (Bearing) Displacement, Base Shear–Displacement Loop, Structure Shear (above Base), Axial Force, and Vertical Uplift Displacement (from Statically Stressed Position) in Bearing above Load Cell LC1; Note that Positive Axial Force Represents Tension Resisted by Uplift Restraints

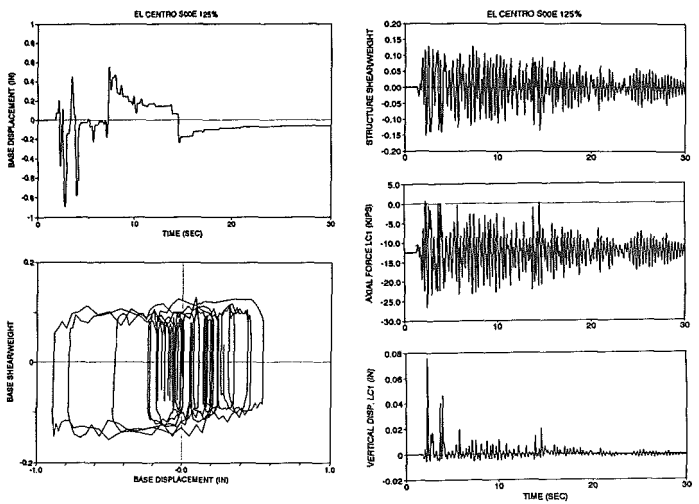

FIG. 4. Measured Response of System with Four Spring Units for El Centro Input with Peak Table Acceleration of 0.41 g; Note that Positive Axial Force Represents Tension Resisted by Uplift Restraints

above the base) time history normalized with respect to the weight (51.4 kips, 228.6 kN); (4) the axial force time history measured by the load cell LC1 (see Fig. 1 for details) below the sliding bearing; and (5) the uplift displacement (from the statically stressed position) recorded at the sliding bearing above load cell LC1. The base shear displacement loop is for the entire system of bearings. The measured time history response for the Pacoima S74W75% excitation shown in Fig. 3 indicates that the uplift displacement exceeded 0.065 in. (1.65 mm) at 2.67 sec and 5.65 sec. Hence, the uplift restraint devices engaged at these instants and carried tensile or uplift forces. The measured response for El Centro S00E 125% excitation shown in Fig. 4 indicates that the uplift displacement exceeded 0.065 in. (1.65 mm) and the uplift restraint devices engaged at 2.27 sec. The uplift restraint devices were not engaged in tests with Mexico City, Hachinohe, Miyagiken-Oki, Taft, or Pacoima S16E excitations, even though loss of contact occurred.

The sliding bearings exhibited stable force-displacement characteristics, despite the large variation of axial or normal forces. Fig. 5 shows the axial force–vertical displacement loop of the bearing on load cell LC1 in the case of El Centro S00E 125% excitation. The axial hysteretic loop shows that the vertical displacement increased from 0.02 in. (0.508 mm) to 0.065 in. (1.65 mm) with zero axial force, after which the engagement of uplift restraint devices resulted in axial force in tension. The loop also shows that the uplift restraint devices engage smoothly. In all tests in which uplift displacement exceeded 0.065 in. (1.65 mm), the uplift restraint devices engaged smoothly.

The higher-mode response of the structure increased in tests in which the uplift restraint devices engaged. The higher-mode response is evident in Fig. 6, which shows the recorded displacement profiles of the model at selected times for the cases with Pacoima S74W 75% and 70%. The times

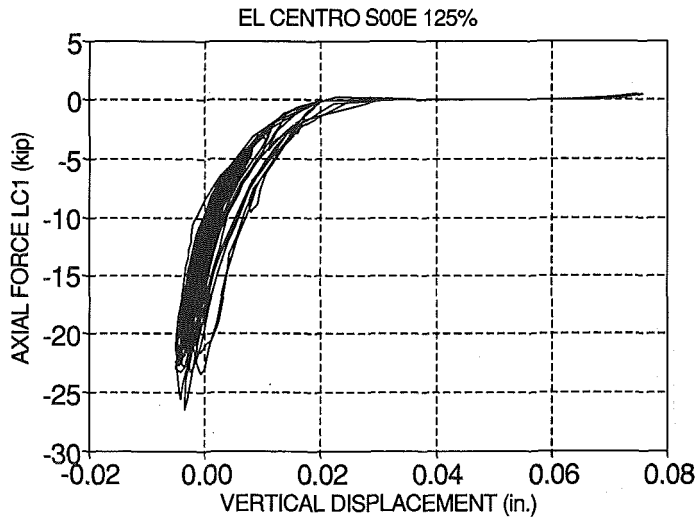

FIG. 5. Axial Force–Vertical Displacement Loop at Sliding Bearing on Load Cell LC1 for El Centro Input with Peak Table Acceleration of 0.41 g; Note Smooth Engagement of Uplift Restraints after Free Uplift (see Fig. 4)

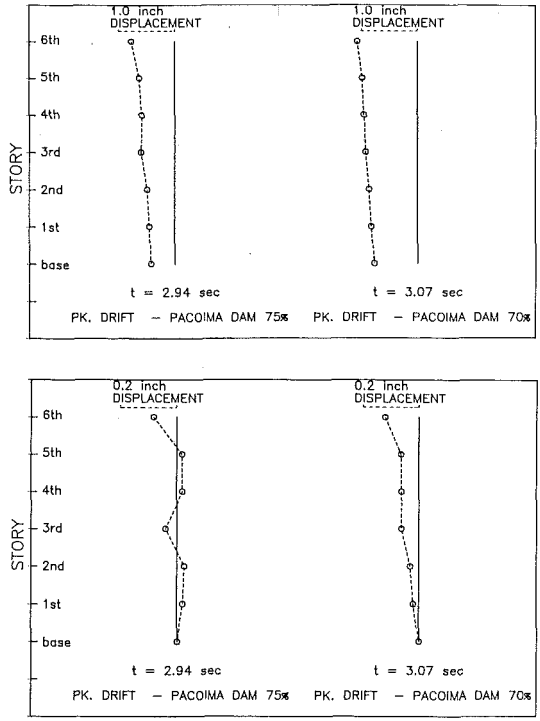

FIG. 6. Profiles of Story Displacement of System with Four Spring Units for Pacoima Dam 75% input with Peak Table Acceleration of 0.58 g and Pacoima Dam 70% input with Peak Table Acceleration of 0.55 g: (a) Displacement Profiles as Recorded; and (b) Displacement Profiles of Superstructure Excluding Rigid Body Base Displacement and Rigid Body Base Rotation due to Rocking; Profiles are Shown at Instants at which Peak Interstory Drift Occurred

at which the profiles are plotted correspond to the instances at which the peak model interstory drift occurred. Fig. 6(*a*) shows the displacement profiles as recorded, and Fig. 6(*b*) shows only the displacement profile of the superstructure, excluding the rigid body base displacement and the rigid body base rotation due to rocking. In the case with Pacoima S74W 75%, uplift restraint devices in the sliding bearings on load cell LC1 (LC4) engaged at 2.67 sec, followed by higher-mode response. This is evident in the displacement profile at the instant at which the peak interstory drift occurred [see Fig. 6(*b*)]. In the case with Pacoima S74W 70%, uplift restraint devices in the sliding bearings on load cell LC1 (LC4) did not engage, even though loss of contact occurred at 2.69 sec (Nagarajaiah et al. 1992), followed by first-mode response. This is evident in the displacement profile at the instant at which the peak interstory drift occurred [see Fig. 6(*b*)]. The vertical acceleration in both cases, close to 3 sec, was within 0.12 g. The peak vertical acceleration due to the uplift and contact was 0.33 g in the test with Pacoima S74W 75%, and less than 0.33 g in all the other tests. In the case with Pacoima S74W 75%, the peak vertical acceleration of 0.33 g occurred after the peak uplift displacement of 0.124 in. (0.315 mm) at 5.65 sec, due to the structure dropping back on to the bearings. The engagement of the uplift

restraint devices, coincidence of peak lateral and rocking response cycles, and the higher-mode response may have been the main cause for the increase in the normalized interstory drift from 0.0016 in the case with Pacoima S74W 70% to 0.0027 in the case with Pacoima S74W 75%.

The measured responses for Hachinohe NS 150% excitation and Miyagken-Oki EW 300% excitation are shown in Figs. 7 and 8. Hachinohe is a low-frequency motion and Miyagiken-Oki is a high-frequency motion. In both cases, the uplift restraints did not engage. Large base displacement of

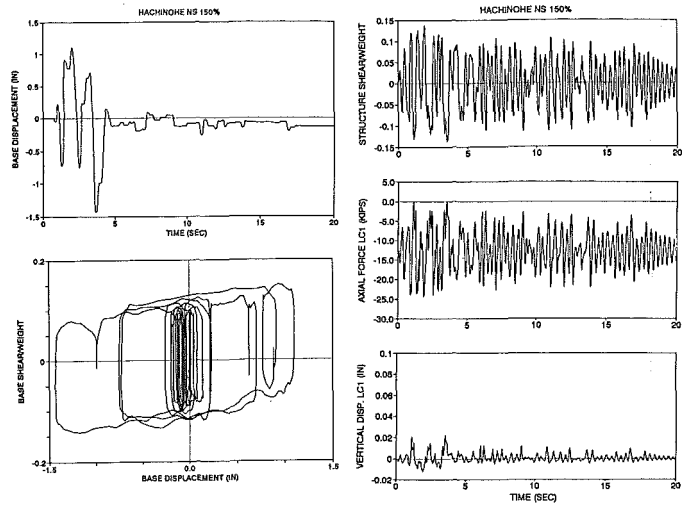

FIG. 7. Measured Response of System with Four Spring Units for Hachinohe Input with Peak Table Acceleration of 0.31 g

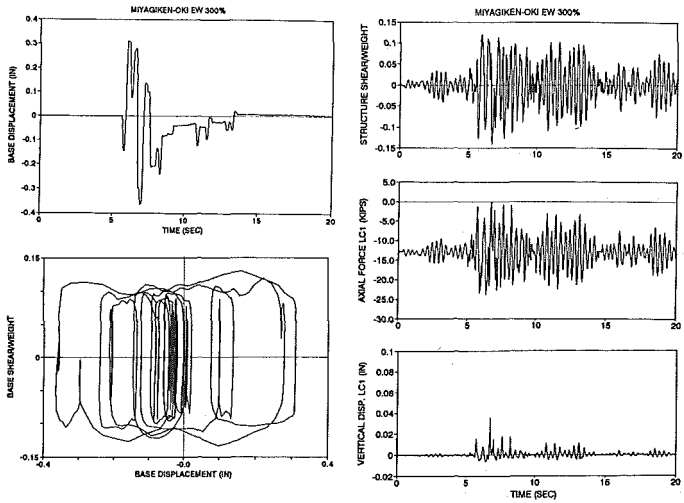

FIG. 8. Measured Response of System with Four Spring Units for Miyagiken-Oki Input with Peak Table Acceleration of 0.46 g

1.43 in. (3.63 mm) occurred in the case with Hachinohe NS 150% excitation, with large variation of axial force, yet the permanent displacement was only 0.13 in. (0.33 mm). The permanent displacement was within 6% of the bearing design displacement of 2.8 in. (71.1 mm) in all tests of the system with four spring units. The interested reader is referred to Nagarajaiah et al. (1992) for a more detailed presentation of results.

Analytical Prediction of Response

An analytical model to predict the response of the structure on the sliding isolation system is presented. The structure is assumed to rest on sliding bearings supported by Adiprene discs. Rocking about the base and the variation of axial forces on the sliding bearings are accounted for. It is assumed that no loss of contact occurs at the sliding inteface. A linear superstructure with a nonlinear isolation system is considered. Furthermore, a lumped mass model with lateral degrees of freedom at the base and all floors is considered. An additional rocking degree of freedom is considered only at the rigid base.

The equations of motion are

$$\mathbf{M}_{n\times n}\ddot{\mathbf{u}}_{n\times 1} + \mathbf{C}_{n\times n}\dot{\mathbf{u}}_{n\times 1} + \mathbf{K}_{n\times n}\mathbf{u}_{n\times 1} = -\mathbf{M}_{n\times n}\mathbf{R}_{n\times 6}(\ddot{\mathbf{u}}_g + \ddot{\mathbf{u}}_b)_{6\times 1} \quad \ldots . (3)$$

$$\mathbf{R}^T_{2\times n}\mathbf{M}_{n\times n}[\ddot{\mathbf{u}} + \mathbf{R}(\ddot{\mathbf{u}}_b + \ddot{\mathbf{u}}_g)]_{n\times 1} + \mathbf{M}_{b2\times 2}(\ddot{\mathbf{u}}_b + \ddot{\mathbf{u}}_g)_{2\times 1} + \mathbf{F}_{f2\times 1} + \mathbf{F}_{r2\times 1} = 0 \quad .. (4)$$

where $\mathbf{M}$, $\mathbf{C}$ and $\mathbf{K}$ = the mass, damping, and stiffness matrices of the superstructure, respectively; $\mathbf{M}_b$ = the diagonal mass matrix containing the mass of the base, and the rotational inertia of the base and the different floors; $\mathbf{R}$ = matrix of earthquake influence coefficients, i.e., the matrix of displacements at different floors due to a unit translation in the horizontal direction and a unit rotation at the base; $\mathbf{U}$ = the vector of floor displacements with respect of the base; $\mathbf{U}_b$ = the vector of lateral base displacement and rotation at the base with respect to the shake table; $\mathbf{U}_g$ = vector of table displacement and rotation; and a dot denotes a differentiation with respect to time. Eq. (3) is the equation of motion for the six-story superstructure, and (4) is the equation of dynamic equilibrium of the entire structure, in the horizontal and rocking directions, about the base. Eqs. (3) and (4) are further reduced using the fixed-base mode shapes normalized with respect to the superstructure mass matrix (Nagarajaiah et al. 1991a, 1991b). In the reduced form, the fixed-base mode shapes, frequencies, and damping ratios (see Table 1) determined experimentally are used.

$\mathbf{F}_f$ and $\mathbf{F}_r$ are the frictional and restoring or recentering force vectors, respectively, at the isolation level. The frictional force vector is given by

$$\mathbf{F}_f = \begin{Bmatrix} [\mu \cos\delta - \text{sgn}\,(U_b)\sin\delta]WZ \\ 0 \end{Bmatrix} \quad \ldots\ldots\ldots\ldots\ldots\ldots\ldots\ldots (5)$$

where sgn stands for the signum function; μ = the coefficient of sliding friction of the Teflon bearing, which depends on the velocity of sliding in accordance with (2) and the bearing pressure; and δ = the accidental average inclination of the sliding interface, which is determined to be 0.5°. Effectively, the mobilized frictional force is lower when the sliding occurs in the downhill direction, and it is larger when sliding occurs in the uphill direction. The inclination of the sliding bearing is of considerable importance (Constantinou et al. 1991). Z in (5) is used to account for the conditions of

separation and reattachment (Constantinou et al. 1990) and is governed by the following differential equation:

$$Y\dot{Z} + \gamma|\dot{U}_b|Z|Z| + \beta\dot{U}_b Z^2 - \dot{U}_b = 0 \quad \ldots\ldots\ldots\ldots\ldots\ldots\ldots\ldots\ldots\ldots (6)$$

where $Y = 0.005$ in. (0.0127 mm) and $\beta + \gamma = 1$.

The restoring force vector is given by

$$\mathbf{F}_r = \begin{Bmatrix} K_{bl}U_b \\ K_r\theta_b \end{Bmatrix} \quad \ldots\ldots\ldots\ldots\ldots\ldots\ldots\ldots\ldots\ldots\ldots\ldots\ldots\ldots\ldots\ldots (7)$$

where K_r = the linear rotational stiffness about the base due to the vertical flexibility of the Adiprene discs and K_{bl} = the bilinear spring stiffness of the helical spring units. The rotational stiffness $K_r = 120{,}000$ kips-ft/rad (162,763 MN-mm/rad) and the bilinear stiffness K_{bl}, for the system with four helical spring units, is as described earlier.

The solution algorithm consists of solving the equations of motion in the incremental form using the pseudoforce method (Nagarajaiah 1991a). The two-step solution algorithm consists of solution of equations motion using: (1) Newmark's unconditionally stable average acceleration method; and (2) solution of the differential equations governing the conditions of separation and reattachment by the unconditionally stable, semi-implicit Runge-Kutta method suitable for solution of stiff differential equations. Furthermore, a iterative procedure consisting of corrective pseudoforces is employed within each time step until equilibrium is achieved. The solution algorithm has been implemented in the computer program 3D-BASIS (Nagarajaiah et al. 1991a, 1991b).

Figs. 9 and 10 show the analytically predicted response for Hachinohe NS 150% and Miyagiken-Oki EW 300% earthquakes. A comparison of the experimental (Figs. 7 and 8) and analytical results (Figs. 9 and 10) reveals the accuracy of the analytical prediction. Almost all details in the observed response are reproduced in the analytical prediction.

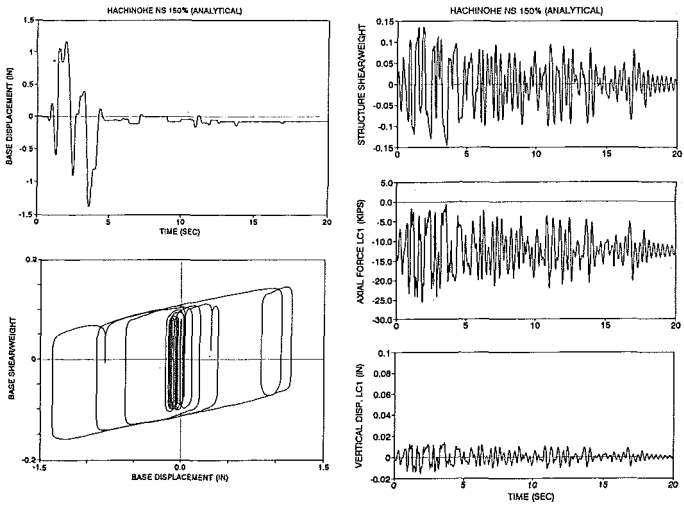

FIG. 9. Computed Response of System with Four Spring Units for Hachinohe Input with Peak Table Acceleration of 0.31 g; Compare with Fig. 7

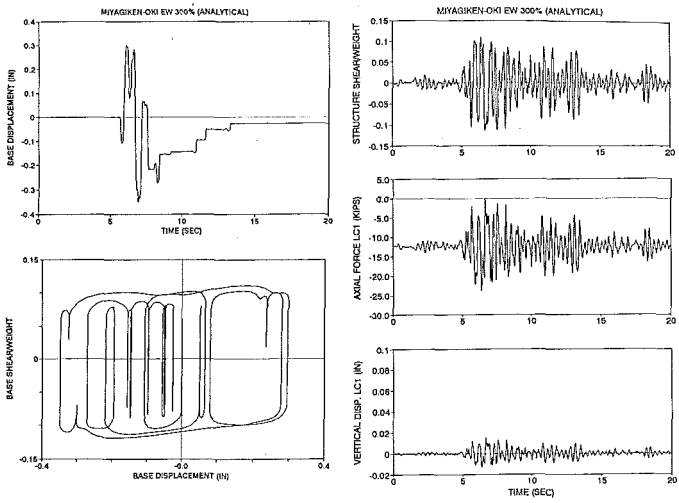

FIG. 10. Computed Response of System with Four Spring Units for Miyagiken-Oki Input with Peak Table Acceleration of 0.46 g; Compare with Fig. 8

CONCLUSIONS

Shake-table tests were performed on a quarter-scale model of a six-story steel-braced frame in which the ratio of height to width was 4.5. The model was isolated using a sliding isolation system. The sliding isolation system consisted of sliding bearings with devices capable of providing uplift restraint. The slender configuration, with aspect ratio of 4.5 considered, resulted in large variation of axial forces on bearings, but no adverse effect was observed.

The following conclusions are derived from the experimental study:

1. The sliding isolation system was effective in reducing the structural response and uplift forces, and the uplift restraint system was effective in resisting uplift forces.
2. The system performed well under motions with significantly different frequency content, ranging from high-frequency motion like the 1940 El Centro to low-frequency motion like the 1985 Mexico City motion.
3. The uplift restraint system performed well even under strong motions like the 1940 El Centro and 1971 Pacoima, with peak table accelerations as high as 0.6 g.
4. The capacity of the frame with a sliding isolation system to withstand the El Centro and Pacoima ground motions, while remaining elastic, was increased by at least a factor of three, compared with the fixed-base case.
5. The response of the system could be reliably predicted by analytical techniques.

ACKNOWLEDGMENTS

The writers wish to acknowledge the financial support provided by the National Center for Earthquake Engineering Research (grant 90-2102), which is supported by the National Science Foundation and the state of New York,

for this project. The writers also wish to acknowledge the assistance of Watson Bowman Acme Corp., Amherst, New York, and GERB Vibration Control, Westmont, Illinois, and the assistance provided by graduate student Ketan Shah in data processing.

APPENDIX. REFERENCES

Beck, J. L., and Skinner, R. L. (1974). "The seismic response of reinforced concrete bridge piers designed to step." *Earthquake Engrg. Struct. Dyn.*, 2(4), 343–358.

Buckle, I. G., and Mayes, R. L. (1990). "Seismic isolation history, application and performance: A world overview." *Earthquake Spectra*, 6(2), 161–202.

Chopra, A. K., and Yim, S. C.-S. (1985). "Simplified earthquake analysis of structures with foundation uplift." *J. Struct. Engrg.*, ASCE, 111(4), 906–930.

Constantinou, M. C., Mokha, A. S., and Reinhorn, A. M. (1990). "Teflon bearings in base isolation II: Modeling." *J. Struct. Engrg.*, ASCE, 116(2), 455–474.

Constantinou, M. C., Mokha, A. S., and Reinhorn, A. M. (1991). "Study of sliding bearing and helical-steel-spring isolation system." *J. Struct. Engrg.*, ASCE, 117(4), 1257–1275.

Griffith, M. C., Aiken, I. D., and Kelly, J. M. (1990). "Displacement control and uplift restraint for base isolated structures." *J. Struct. Engrg.*, ASCE, 116(4), 1135–1148.

Housner, G. W. (1963). "The behavior of inverted pendulum structures during earthquakes." *Bull. Seismol. Soc. Am.*, 53(2), 403–417.

Huckelbridge, A. A., and Clough, R. W. (1978). "Seismic response of uplifting building frames." *J. Struct. Engrg.*, ASCE, 104(8), 1211–1229.

Kelly, J. M. (1988). "Base isolation in Japan, 1988." *Report No. UCB/EERC-88/20*, Earthquake Engrg. Res. Ctr., Univ. of California, Berkeley, Calif.

Meek, J. W. (1975). "Effects of foundation tipping on dynamic response." *J. Struct. Engrg.*, ASCE, 101(7), 1297–1311.

Nagarajaiah, S., Reinhorn, A. M., and Constantinou, M. C. (1992). "Experimental and analytical study of sliding isolated structures with uplift restraint." *Report No. 92-X*, National Ctr. for Earthquake Engrg. Res., State Univ. of New York, Buffalo, New York (in print).

Nagarajaiah, S., Reinhorn, A. M., and Constantinou, M. C. (1991a). "Nonlinear dynamic analysis of 3-D base isolated structures." *J. Struct. Engrg.*, ASCE, 117(7), 2035–2054.

Nagarajaiah, S., Reinhorn, A. M., and Constantinou, M. C. (1991b). "3D-BASIS: Nonlinear dynamic analysis of three dimensional base isolated structures." *Report No. 91-0005*, National Ctr. for Earthquake Engrg. Res., State Univ. of New York, Buffalo, N.Y.

Priestly, M. J. N., Evison, R. J., and Carr, A. J. (1978). "Seismic response of structures free to rock on their foundations." *Bull. New Zealand Nat. Soc. Earthquake Engrg.*, 11(1), 141–150.

Psycharis, I. N. (1990). "Effect of base uplift on dynamic response of SDOF structures." *J. Struct. Engrg.*, ASCE, 117(3), 733–753.

Wabo-Fyfe High Load Structural Bearing. (1990). Watson Bowman Acme Corporation, Amherst, N.Y.

Wolf, J. P. (1976). "Soil-structure interaction with separation of base mat from soil (lifting-off)." *Nucl. Engrg. Des.*, 38(2), 357–384.

Zayas, V., Stanley, L., Bozzo, L., and Mahin, S. (1989). "Feasibility and performance studies on improving the earthquake resistance of new and existing buildings using the friction pendulum system." *Report No. UCB/EERC-89/09*, Earthquake Engrg. Res. Ctr., Univ. of California, Berkeley, Calif.